Volume 267, Issues 3–4 30 March 2008 ISSN 0012-821X

EARTH & PLANETARY SCIENCE LETTERS

Available online at www.sciencedirect.com
ScienceDirect
Earth and Planetary Science Letters 267 (2008) 558–570
EPSL
www.elsevier.com/locate/epsl

Field evidence of Eros-scale asteroids and impact-forcing of Precambrian geodynamic episodes, Kaapvaal (South Africa) and Pilbara (Western Australia) Cratons

Andrew Y. Glikson *

Research School of Earth Science and Planetary Science Institute, Australian National University, Canberra, A.C.T. 0200, Australia

Received 8 April 2007; received in revised form 28 November 2007; accepted 2 December 2007
Available online 29 January 2008
Editor: G.D. Price

Abstract

The role of asteroid and comet impacts as triggers of mantle–crust processes poses one of the fundamental questions in Earth science. I present direct field evidence for close associations between impact ejecta/fallout units, major unconformities and lithostratigraphic boundaries in Archaean and early Proterozoic terrains, including abrupt changes in the composition of volcanic and sedimentary assemblages across stratigraphic impact boundaries, with implications for the nature and composition of their provenance terrains. As originally observed by D.R. Lowe and G.R. Byerly, in the Barberton Greenstone Belt, eastern Kaapvaal Craton, South Africa, 3.26–3.24 Ga asteroid mega-impact units are closely associated with the abrupt break between an underlying simatic mafic–ultramafic volcanic crust and an overlying association of turbidites, banded iron formations, felsic tuff and conglomerates of continental affinities. Contemporaneous stratigraphic relationships are identified in the Pilbara Craton, Western Australia. Evidence for enrichment of seawater in ferrous iron in the wake of major asteroid impacts reflects emergence of new source terrains, likely dominated by mafic compositions, attributed to impact-triggered oceanic volcanic activity. Relationships between impact and volcanic activity are supported by the onset of major mafic dyke systems associated with ~2.48 Ga and possibly the 2.56 Ga mega-impact events.

Keywords: asteroid; impact; microkrystites; crustal evolution; Archaean; early Proterozoic

1. Introduction

The role of large asteroid and comet impacts as triggers of major tectonic, plate tectonic, thermal, magmatic and environmental episodes (Price, 2001; Green, 1981; Grieve, 1980; Hughs et al., 1977; Jones, 1987; Jones et al., 2002; Jones et al., 2005; Alt et al., 1988; Oberbeck et al., 1992; Boslough et al., 1994; Glikson, 2001; Glikson, 2005; Glikson, 2006; Ingle and Coffin, 2004; Ivanov and Melosh, 2003; Glikson et al., 2004a,b; Elkin-Tanton et al., 2004; Elkin-Tanton and Hager, 2005) constitutes a fundamental question in Earth science. D.R. Lowe and G.R. Byerly (Lowe et al., 1989; Lowe and Byerly, 1990) identified a juxtaposition between three 3.26 and 3.24 Ga impact ejecta/fallout units (S2, S3, S4) in the Barberton Greenstone Belt (BGB), eastern Kaapvaal Craton, South Africa, and the abrupt break between (A) 3.55 and 3.26 Ga mafic–ultramafic volcanic crust (Onverwacht Group and Mendon Formation) (Figs. 1, 2) and unconformably overlying <3.26 Ga turbidite, banded iron formation (BIF), felsic volcanic, and conglomerate-dominated continental type association (Fig Tree Group, Moodies Group), which includes the earliest observed granite derived detritus. Glikson and Vickers (2006) correlated the BGB 3.26–3.24 Ga impacts with contemporaneous stratigraphic units in the Pilbara Craton, Western Australia (Fig. 3). Here an abrupt break occurs between a 3.51–3.235 Ga mafic–ultramafic sequence (Cooterunah, Warrawoona and Sulphur Springs Groups, Pilbara Craton) and a <3.235 Ga turbidite–felsic volcanic–BIF association and overlying conglomerates (Gorge Creek Group, de Grey Group), a boundary

* Tel./fax: +61 2 6196 3853.
E-mail address: andrew.glikson@anu.edu.au.

0012-821X/$ - see front matter © 2007 Elsevier B.V. All rights reserved.
doi:10.1016/j.epsl.2007.12.007

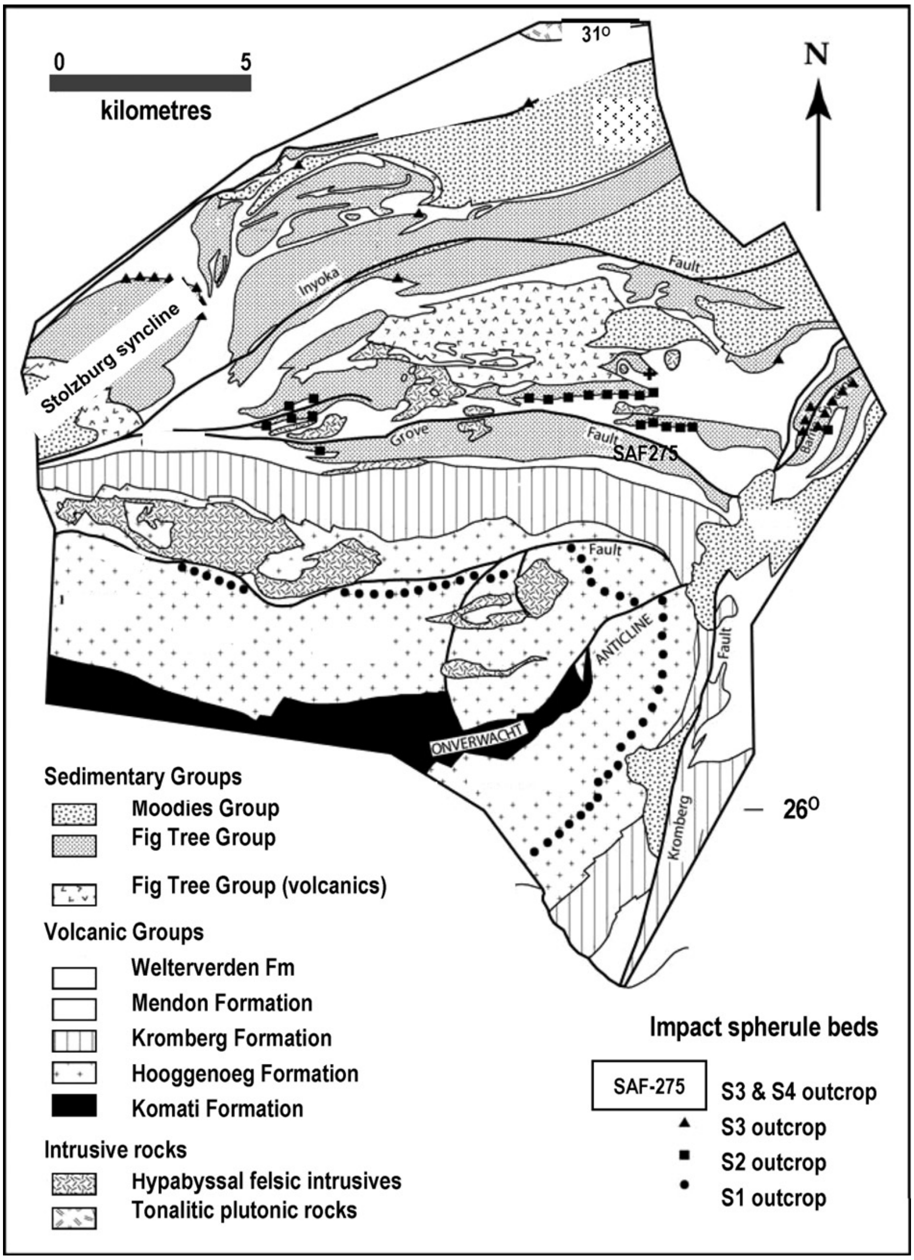

Fig. 1. Geological sketch map of the SW Barberton Greenstone Belt, east Kaapvaal Craton, South Africa, showing distribution of the S1, S2, S3 and S4 Impact spherule units (Lowe et al., 2003) (courtesy D.R. Lowe and G.R. Byerly).

accompanied by multiple olistostromes overlain by siltstone and ferruginous sediments (Fig. 4). A similar break occurs in the western Pilbara Craton at ~3.27–3.25 Ga.

The significance of ferruginous argillite, jaspilite and BIF which overlie 3.46, 3.26, 3.24, 2.63 and 2.56 Ga-old impact ejecta/fallout units in the Pilbara and Kaapvaal Craton was considered in terms of changes in provenance terrains associated with tectonic and magmatic effects of these impacts (Glikson, 2006). Here I elucidate the field evidence for geodynamic episodes triggered by impacts by Eros-scale (D~30 km) asteroids in Archaean to early Proterozoic terrains, with implications for the structure and evolution of the Archaean and early Proterozoic Earth. Criteria for the identification of extraterrestrial impact ejecta units include presence of microkrystite spherules (Glass and Burns, 1988) which display inward-radiating quench textures, central-offset vesicles, relic nickel-rich spinels, high siderophile and platinum group elements (PGE) (Byerly and Lowe, 1994), high Ni/Cr and Ir/Pd ratios (Glikson, 2007) and anomalous Cr isotopic ratios (Shukolyukov et al., 2000; Kyte et al., 2003). Impact ejecta units may be conformable, transgress different facies boundaries or overlie unconformities (Lowe et al., 1989; Lowe and Nocita, 1999; Lowe et al., 2003). Quench-textured Ni-chromites (NiO<23%) with high Co, Zn and V abundances display disequilibrium crystallization and may contain nickel-rich and PGE-rich micronuggets (Glikson, 2005; Glikson, 2007). Chondrite-normalized patterns display a marked depletion in the volatile PGE species (Pd, Au) relative to refractory

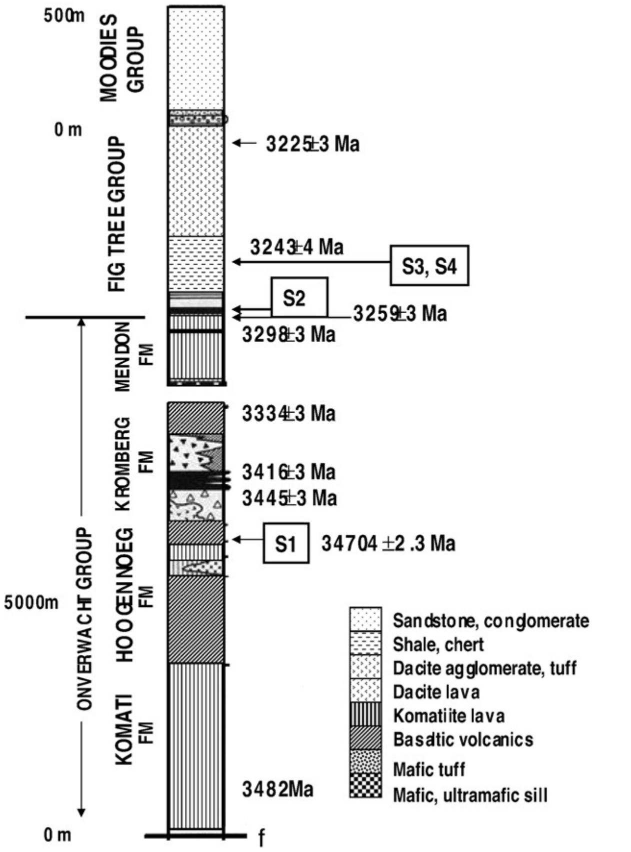

Fig. 2. Schematic stratigraphic section and isotopic ages of the Onverwacht Group and Fig Tree Group, Barberton Greenstone Belt.

species [Ir, Pt) which, excepting depleted mantle harzburgite, are distinct from terrestrial PGE profiles (Glikson, 2007). Negative $^{53}Cr/^{52}Cr$ isotopic indices correspond to values of carbonaceous chondrites and K–T boundary impact fallout unit (Shukolyukov et al., 2000; Kyte et al., 2003).

2. The 3.26–3.24 Ga impact cluster

In the Barberton Greenstone Belt (BGB), eastern Kaapvaal Craton, the ~3.26 Ga S2 impact unit coincides with the base of the clastic Mapepe Formation of the Fig Tree Group. The ~3.24 Ga S3 and S4 impact units occur within clastic sediments and felsic pyroclastics 110–120 m above the basal contact of the Fig Tree Group. In places the S3 impact unit is unconformable, cutting into underlying Mendon Formation komatiites. The ~3.26 Ga S2 impact ejecta unit is overlain by 20-to 30-m-thick banded ferruginous chert of the basal Mapepe Formation (Lowe and Nocita, 1999; Lowe et al., 2003). These iron-rich sediments, termed Manzimnyama Jaspilite Member, include oxide facies BIF, jaspilite, hematite-rich shale and shale located at lowermost stratigraphic levels of the Mapepe Formation. In the southern part of the BGB the jaspilite is either separated from the S2 unit by up to 50 m of terrigenous sediments and felsic pyroclastics, or directly overlies the S2 impact unit. In the northern part of the Barberton Greenstone Belt the ~3.24 Ga S3 impact spherule unit underlies iron-rich sediments of the Ulundi Formation, including jaspilite, ferruginous chert and black chert deposited under quiet deep-water conditions. By contrast deposition of S2 and S3 unit in the Onverwacht anticline zone, which formed an antecedent rise located between the deeper basins to the northwest and southeast, took place under high-energy shallow-water conditions, which likely precluded colloidal precipitation of iron and silica, which may account for the lack of iron-rich sediments in this sector (Lowe et al., 2003).

Evidence consistent with potential magmatic consequences of the Barberton impact cluster is provided by U–Pb zircon ages

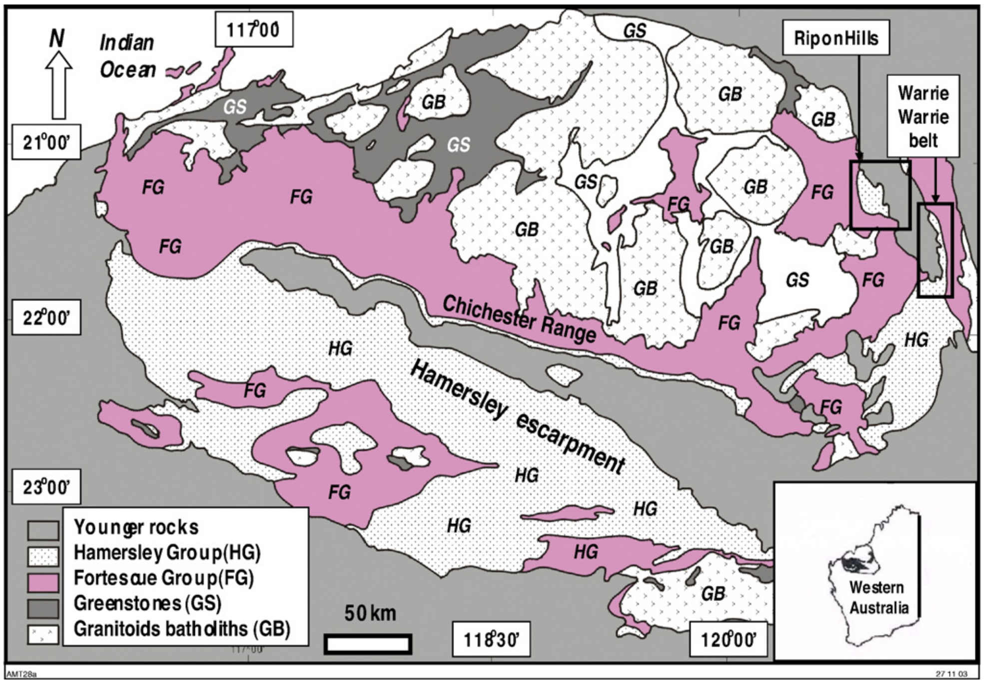

Fig. 3. Geological sketch map of the Pilbara Craton and Hamersley Basin.

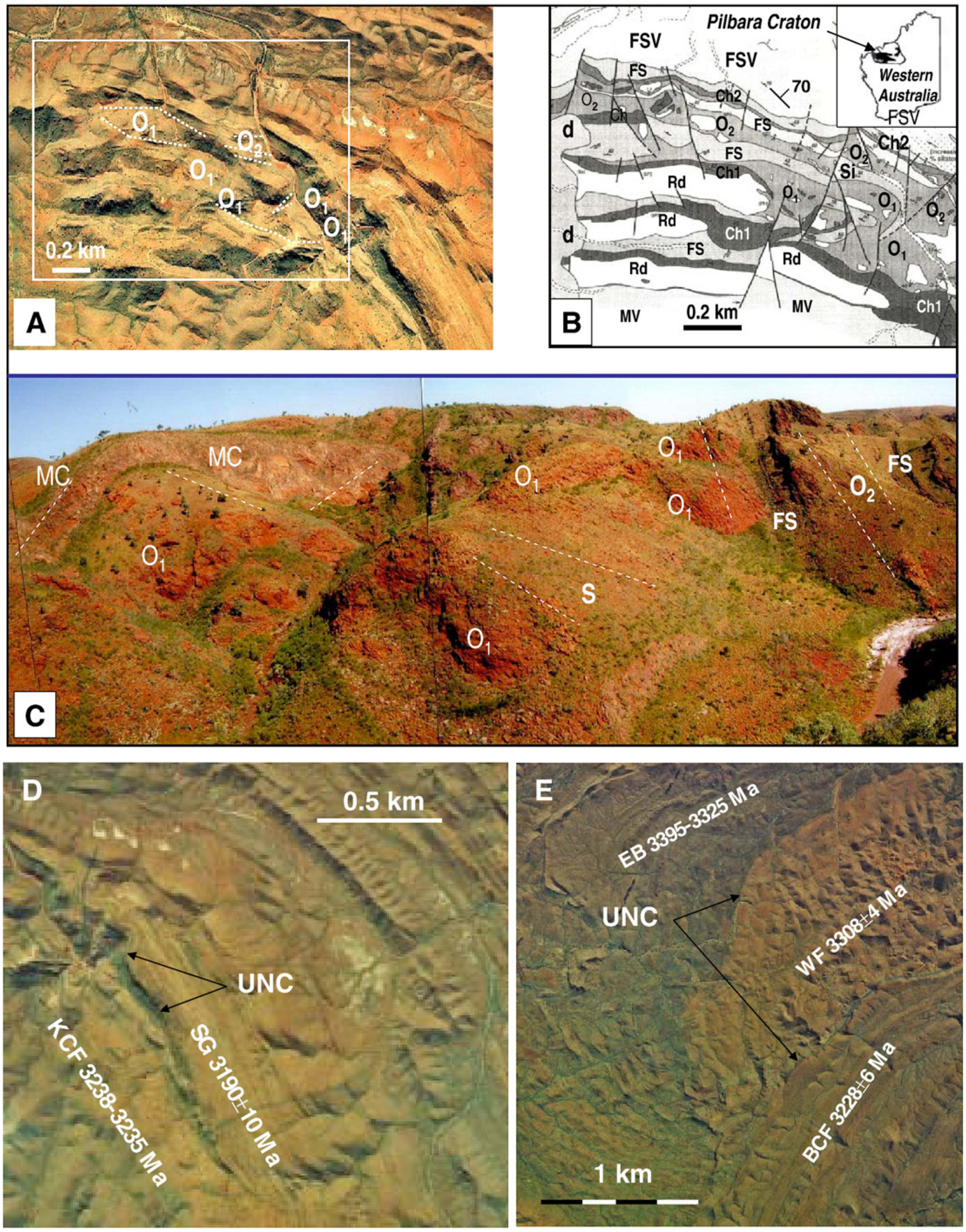

Fig. 4. Olistostromes of the Sulphur Springs area, central Pilbara Craton. (A) Aerial photograph of part of the Sulphur Springs area, central Pilbara Craton. O1 — lower olistostrome; O2 — upper olistostrome. For other geological units refer to part B, defined by the framed area in the aerial photograph. (B) Geological map of part of the Sulphur Springs area (after (Hill, 1977)). MV — mafic volcanics of the Sulphur Springs Group; Rd — rhyodacite sills emplaced in the SSG; FS — ferruginous siltstone; Ch1 — Marker Chert at the top of the SSG; Ch2 — chert at the top of the upper Olistostrome; O1 — lower olistostrome; O2 — upper olistostrome; FSV — ferruginous siltstone including felsic pyroclastics; d — dolerite. (C) Photo-panorama showing the top Marker Chert of the Sulphur Springs Group (MC), olistostromes (O1 and O2) and overlying ferruginous sediments (FS) and siltstone (S), looking southwest across Sulphur Springs Creek. (D) Aerial photograph displaying the unconformity between the Kangaroo Cave Formation (KCF: 3235±5 Ma), top Sulphur Springs Group (3255–3235 Ma) and conglomerate and quartzite of the Soanesville Group (SG: 3190±10 Ma). UNC — unconformity. (E) Aerial photograph displaying high-angle unconformity between the Wyman Rhyolite (WR: 3308±4 Ma) and the Budjan Creek Formation (BCF: 3228±6 Ma), Kelly greenstone belt. UNC — unconformity.

of the Nelshoogte trondhjemite (3236±1 Ma) and the Kaap Valley tonalite (3227±1 Ma), which closely follow the S3 and S4 impact units (3243±4 Ma). The high precision of these U–Pb zircon ages may imply that anatexis, segregation and rise of plutonic magmas occurred within ~5–10.10^6 yrs from the S3 and S4 impacts. The tonalite–trondhjemite geochemistry of the granitoids suggests anatexis involved mainly mafic crustal rocks.

In the Sulphur Springs area, central Pilbara Craton (Fig. 4A, B), stratigraphic levels closely correlated with the BGB sequence which hosts the S2–S4 impact units include the mafic to felsic volcanic Sulphur Springs Group (SSG: ~3255–3235 Ma) and unconformably overlying conglomerate and arenite (Soanesville Group: 3190±10), argillite, banded iron formation and felsic tuff of the Pincunah Hill Formation (PHF) of the Gorge Creek Group (Glikson and Vickers, 2006; Van Kranendonk, 2000; Van Kranendonk et al., 2002; Van Kranendonk et al., 2005; Van Kranendonk et al., 2006; Buick et al., 2002; Hill, 1977). Locally a major olistostrome lens ~600 m thick overlies the unconformity, consisting of two to three boulder to mega-boulder debris flows containing up to 250 m-large blocks of chert, argillite and felsic volcanics (Hill, 1977). Each debris flows is overlain by ferruginous argillite and chert (Fig. 4C). Low-angle post-SSG unconformity is displayed in the Sulphur Springs area (Fig. 4D) and high-angle unconformity in Kelly greenstone belt, where the Budjan Creek Conglomerate overlies mafic volcanics with a high angular unconformity over Wyman Formation felsic volcanics (3308±4 Ma) and Euro Basalt mafic volcanics (3395–3325 Ma) (Fig. 5E) (Fig. 4E).

The following correlations pertain between the BGB S2–S4 impact fallout units and stratigraphic units in the central Pilbara Craton (Fig. 5):

(A) The Leilira Formation (LF) — which consists of a basal conglomerate, silici-clastic arenite, argillite, and felsic volcanics dated as 3255±3 Ma at the base of the 2500–3000 m thick SSG (Buick et al., 2002), correlates with the 3258±3 Ma BGB-S2 impact ejecta unit. The LF unconformably overlies volcanics of the 3.35–3.30 Ga Kelly Group. The overlying komatiites and basalt of the Kunagunarrina Formation are in turn overlain by basalt–andesite–rhyolite of the 3235±5 Ma Kangaroo Cave Formation (KCF), capped by a marker chert composed of fine grained epiclastic and silici-clastic rocks. The SSG is intruded by the co-magmatic 3238±3 Ma Strelley Monzogranite laccolith.

(B) The 3235±5 Ma KCF is overlain unconformably by conglomerate, quartzite, turbidite, felsic volcanics and banded iron formations of the Soanesville Group and the Gorge Creek Group. The unconformity is correlated with stratigraphic discontinuities associated with the 3243±4 Ma S3 and S4 impact units of the Mapepe Formation, BGB. In the Soanesville area the SSG is overlain by chert, in turn overlain by arenite and micro-conglomerate of the Cardinal Formation (Van Kranendonk et al., 2005).

Arenites of the Soanesville Group unconformably overlap and cut into the marker chert at the top of the SSG, indicating older faulting. The Pincunah Hill Formation (PHF) of ferruginous shale and felsic volcanics is overlain by BIF and ferruginous shale of the Paddy Market Formation (PMF) (Van Kranendonk, 2000). As in the Barberton Greenstone Belt, end-SSG felsic volcanism is accompanied with major plutonic activity which produced ~3.25–3.235 Ga granitoids of the Cleland Supersuite in central parts of the Mount Edgar, Muccan and Warrawagine batholiths (east Pilbara), Carlindi batholith, Strelley Granite and Tambourah Monzogranite (central Pilbara). In the west Pilbara Craton the break between mafic volcanics of the Roebourne Group (Ruth Well Formation) and silici-clastic deposits (Nickol River Formation) may be somewhat older at 3.27–3.25 Ga, and is likewise accompanied by plutonic activity (3.27–3.26 Ga Karratha Granodiorite) (Van Kranendonk et al., 2002). The BIF units of the Gorge Creek Group may correspond

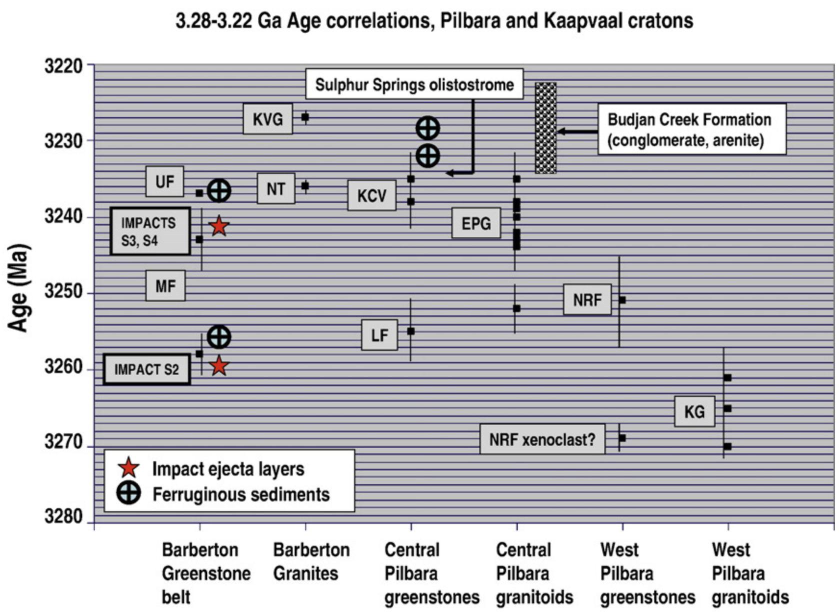

Fig. 5. Isotopic age correlations between 3.28 and 3.22 Ga units in the Kaapvaal Craton and Pilbara Craton. Solid squares and error bar lines — U–Pb ages of volcanic and plutonic units; stars — impact ejecta layers; circled crosses — ferruginous sediments; MF — Mapepe Formation; UF — Ulundi Formation; NT — Nelshoogte tonalite; KVG — Kaap Valley Granite; LF — Leilira Formation; KCV — Kangaroo Cave volcanics; EPG — Eastern Pilbara granites; NRF — Nickol River Formation (including an older xenoclast); KG — Karratha Granite.

to the 3243±4 Ma to 3225±3 Ma age range of BIFs of the Mapepe Formation of the Barberton Greenstone Belt.

Despite a long search in outcrop and drill cores, no impact ejecta have been identified at the base of the Leilira Formation or the Soanesville Group. Had microkrystite spherules settled in these quartz rich conglomerates and arenites, they would have been corroded and crushed in the high-energy environment.

3. Significance of iron enrichment of sea water associated with asteroid mega-impact events

The ~3.47 Ga impact fallout unit of the central Pilbara Craton (Lowe et al., 1989; Byerly et al., 2002; Glikson et al., 2004a,b), hosted by the Antarctic Chert Member at the base of the Apex Basalt, Warrawoona Group, is overlain by a distinct regional jaspilite marker unit which can be traced around the North Pole dome (Van Kranendonk, 2000). The jaspilite, correlated with the Marble Bar Chert of the Towers Formation, near Marble Bar, varies in thickness from under 0.5 m in the western part of the North Pole dome to a total of over 10 m in the eastern part of the North Pole dome to near-100 m in the Marble Bar area about 40 km to the east. The jaspilite is intercalated with carbonated felsic to intermediate tuffs and derived sediments. No iron-rich sediments are reported from above the contemporaneous S1 impact spherule unit of the Hooggenoeg Formation, Barberton Greenstone Belt (Lowe et al., 2003).

The identification of the Jeerinah Impact Layer (JIL), a 6 mm-thick lamina of microkrystite spherules above argillite–chert sequence of the Jeerinah Formation at Ilbiana Well, was followed by the discovery of an outcrop at Hesta siding, Newman–Port Hedland railway line (Simonson and Glass, 2004; Hassler et al., 2005; Glikson, 2004; Simonson et al., 2000; Simonson and Hassler, 1997). JIL constitutes an up to 60 cm-thick unit of microkrystite spherules and spherule-bearing rip-up clast breccia located above argillite and chert of the Jeerinah Formation and overlain by boulder-size debris flow (Fig. 6). The age of JIL is constrained by U–Pb zircon date of 2629±5 Ma of an overlying volcanic tuff (Trendall et al., 2004) and U–Pb age of 2684±6 Ma from the base of the underlying Jeerinah Formation (Arndt et al., 1991). The age of the overlying Marra Mamba Iron Formation is indicated by a U–Pb zircon age for its uppermost member (Mount Newman Member — MNM) of 2597±5 Ma (Trendall et al., 2004). The age gap of ~20.10^6 yrs between the JIL and MNM signifies long-term deposition of the ferruginous sediments or, more likely, discontinuous deposition and presence of undetected depositional gaps (paraconformities) between the JIL and the banded iron formations or within the Marra Mamba Iron Formation.

A 20–30-m-thick microkrystite and microtektite-bearing carbonate-chert stratiform megabreccia (CMB) unit, identified by Simonson (1992) at the lower part of the Carawine Dolomite, extends over a distance of nearly 100 km northwest–southeast between Ripon Hills and Warrie Warrie Creek, eastern outlier of the Hamersley Basin (Glikson, 2004) (Fig. 3). The megabreccia is located about 30–100 m above the contact with underlying siltstone of the Jeerinah Formation, where crystal tuff was dated as 2630±6 Ma (Rasmussen et al., 2005). The megabreccia is either excavated into, or conformably overlies, layered carbonate (Glikson, 2004), and consists of chert and dolomite fragments and up to 7 m-large blocks derived from the underlying carbonates and chert-rich dolomite. Locally the megabreccia is only ~5–10 m thick. The top of the megabreccia pile is marked by several centimetres-thick lenses of microkrystite spherules and microtektites. Isolated spherules occur within the breccia piles, mainly in downward-injected veins. Carbonate sequences underlying the CMB vary from about 100 m thick in the northwest Ripon Hills, to about 30 m in the southern Ripon Hills, to a few tens of metres in the southern part of the Warrie Warrie belt.

The CMB was initially regarded as a tsunami facies of the ~2.56 Ga Spherule Marker Bed (SMB) of the central Hamersley Basin, due to their associated carbonate facies sediments and Pb isotope age (Simonson, 1992). However, unless the Jeerinah Formation and the CMB are separated by an undocumented depositional gaps, the age overlap between the JIL (2629±5 Ma) and the sub-CMB tuff (2630±6 Ma) militates for a correlation between stratigraphic levels immediately below the Marra Mamba Iron Formation and the base of carbonate facies in the eastern Hamersley Basin (Hassler et al., 2005; Simonson and Hassler, 1997). Alternatively, the JIL and CMB represent separate, though geochronologically indistinguishable, impact events. A possible equivalent of the CMB was identified in the Transvaal Group, West Griqualand Basin, South Africa where an impact layer occurs at lower parts of the thick carbonate sequence of the ~2.6–2.65 Monteville Formation (Simonson et al., 2006). Due to possible depositional gaps within stratigraphic sections in both, the Hamersley Group and the Transvaal Group, as well as errors inherent in the isotopic ages, the inter-continental correlation of the JIL and SMB remains uncertain (Simonson and Glass, 2004), which leaves open the possibility of distinct impact events.

The 2.56 Ga SMB (Simonson, 1992) forms a unique 10–130 cm-thick black-weathering microkrystite and microtektite-bearing turbidite at the top of the ~230 m-thick carbonate–marl–siltstone sequence of the Bee Gorge Member, Wittenoom Formation. It consists of centimetre-scale densely packed spherule layers and discontinuous lenses overlain by decimetre-thick graded and cross-layered turbidite units. The maximum age of the spherules is defined by U–Pb ages on an underlying tuff unit dated as 2565±9 Ma (Trendall et al., 2004). A possible equivalent of the SMB occurs in the ~2567 Ma Reivilo Formation, West Griqualand Basin, Transvaal, located within carbonaceous shale and stromatolitic carbonate about 250–300 m above the Monteville impact layer (Simonson and Glass, 2004; Simonson et al., 2006).

Further studies suggest that the SMB may include two distinct impact cycles, each consisting of a discontinuous basal layer or lenses of spherules overlain by Bouma-cycle turbidites and/or cross-layered tsunami-type calcareous arenite, commonly including turbulence structures (Glikson, 2004). The SMB extend for at least 325 km E–W throughout the Hamersley Basin, over an area ~16000 km^2, showing thickness and facies variations from centimetre-scale layers and

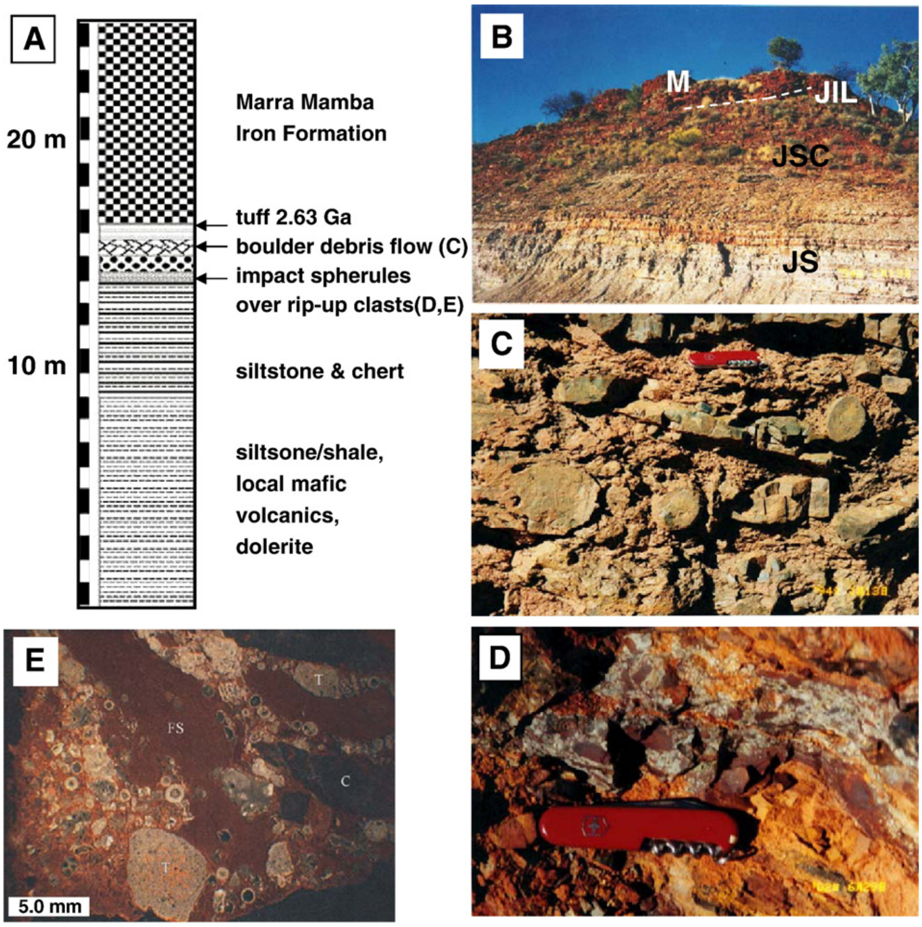

Fig. 6. Jeerinah Impact Layer (JIL), Hesta type section, central Pilbara Craton. (A) Columnar section of the Jeerinah Impact Layer (JIL) and host sediments (Glikson, 2004). (B) Railroad-side exposure at Hesta siding, central Pilbara, showing Jeerinah Formation siltstone (JS) and siltstone–chert (JSC), the Jeerinah Impact Layer (JIL) and laterite-altered base of the Marra Mamba Iron Formation (M). (C) Boulder debris flow above JIL, containing tabular and rounded decimetre-scale fragments. Swiss knife — 8 cm. (D) Basal rip-up clast breccia of JIL consisting of spherule-rich microbreccia (white) containing rip-up clasts of ferruginous siltstone (red). (E) Microscopic view of spherule-rich breccia with rip-up clasts of ferruginous siltstone, showing K-feldspar-rimmed chlorite-cored microkrystite spherules and feldspar-dominated microtektites (large fragment at the bottom). (For interpretation of the references to color in this figure legend, the reader is referred to the web version of this article.)

discontinuous lenses of densely packed spherules in carbonate-argillite matrix to several decimetre-thick turbidite units with or without dispersed spherules. The thickness of spherules generally decreases from north to south and from east to west. Marked variations were observed between fully developed ~1 m-thick spherule-bearing turbidites, comprising two distinct spherule-bearing cycles (SMB-1 and SMB-2), and thin spherule-poor or spherule-free equivalents consisting of one, two or three spherule-bearing and/or spherule-free turbidite units.

Examination of the stratigraphy of the SMB suggests that the impact unit coincides with the boundary between contrasted lithological assemblages (Fig. 7), including:

1. An underlying sequence dominated by carbonate and calcareous siltstone, accompanied with minor shale, chert, felsic tuff (Bee Gorge Member), and locally pockets of intraformational conglomerate and cross-layered turbidites, including rip-up clasts suggestive of tsunami effects. Sections in the Bee Gorge Member below the SMB have a high ratio of calcareous siltstones+carbonate to siltlstone (~10 at Wittenoom Gorge), including banks of near-pure carbonate, which include chert intercalations.
2. An overlying sequence dominated by siltstone, chert, ferruginous chert and minor calcareous sediments, with increasing ferruginous components upward in the sequence (Mount Sylvia Formation). The first few metres of sections overlying the SMB have a ratio of ~2.5 calcareous siltstone and siltstone to carbonate, grading upward into less calcareous siltstone and increasingly ferruginous sediments. At Bee Gorge a calcareous bank about 20 m above the SMB represents the stratigraphically uppermost manifestation of carbonate facies.

The observed spatial and temporal association between Archaean mega-impact ejecta/fallout units, lithological discontinuities, unconformities, increased high-energy clastic sedimentation and appearance of banded iron formations, is suggestive of

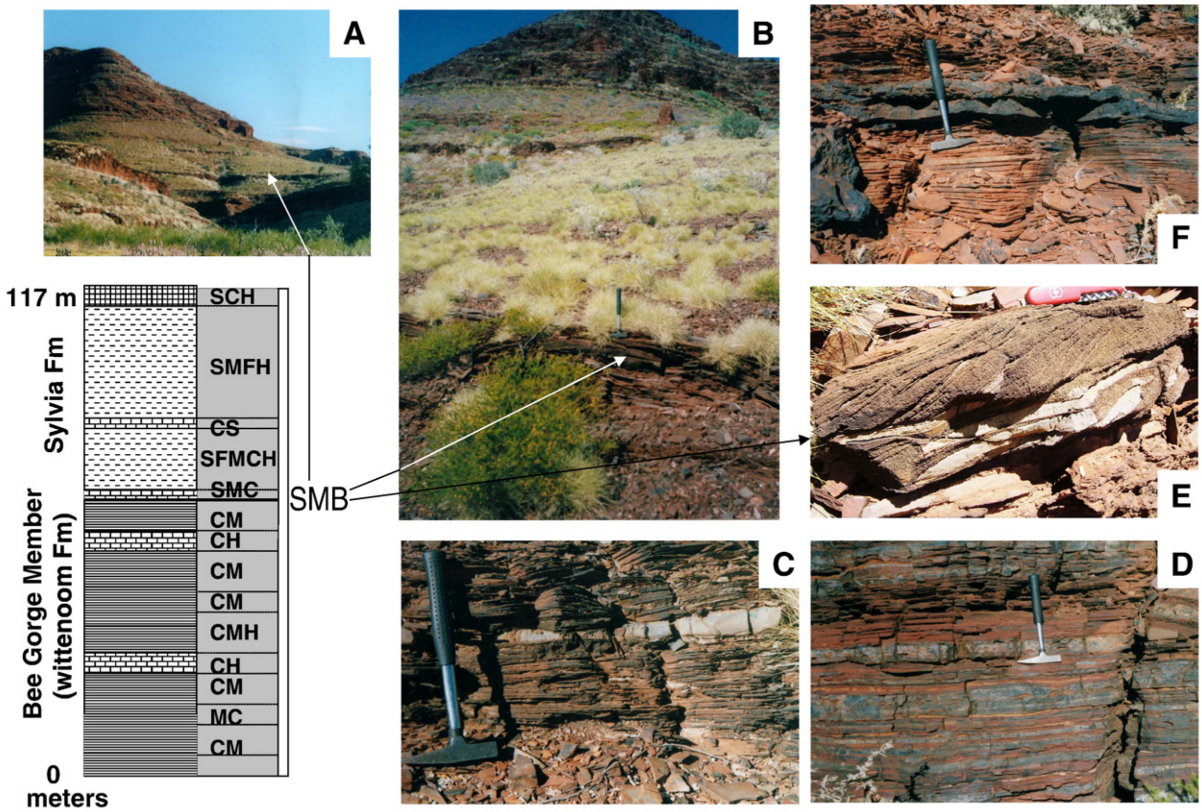

Fig. 7. Bee Gorge section (see Fig. 3). Columnar section and outcrops of the Bee Gorge Member (BGM) of the Wittenoom Formation, Spherule Marker Bed (SMB) and Mount Sylvia Formation; C — carbonate; M — marl and calcareous siltstone; H — chert; S — siltstone; F — ferruginous siltstone and chert. (A) A view of Bee Gorge Creek section east of the opening of Bee Gorge. Arrow points to the location of the SMB. (B) Outcrop of the SMB overlain by siltstone, ferruginous siltstone and minor carbonate. The brown bank at mid-distance is the uppermost carbonate unit in the section, overlain by ferruginous siltstone and Fe-chert. (C) Bee Gorge Member: Calcareous siltstone (marl) including a carbonate layer (white). (D) Bee Gorge Member: carbonates (grey layers) and calcareous siltstone (red). (E) SMB: Microkrystite spherule-bearing cross-layered turbidite. (F) Mount Sylvia Formation: Fe-chert layers (black) within ferruginous siltstone. (For interpretation of the references to color in this figure legend, the reader is referred to the web version of this article.)

rejuvenation of source terrains and of enrichment of sea water in soluble ferrous iron. Barring possible undocumented long-term depositional gaps between the impact layers and the overlying BIF and clastic sediments/BIF association, enrichment in iron has been temporally associated with, and thus possibly related to, the impact events. The absence of ferruginous sediments above impact spherule-bearing Carawine megabreccia, east Hamersley Basin (Simonson, 1992; Glikson, 2004), Monteville and Reivilo impact layers, West Griqualand Basin, Transvaal (Simonson and Glass, 2004; Simonson et al., 2006) may be related to the stromatolitic nature of the host carbonates, which likely formed in partly protected shallow reef environments where high pH alkaline conditions would preclude deposition of banded iron formations.

The origin of iron enrichment above 3.47 Ga, 3.26 Ga, 3.24 Ga, 2.63 Ga and 2.56 Ga impact layers and their associated tsunami deposits may be interpreted in terms of mafic volcanic and Fe-rich hydrothermal activity triggered by the impacts (Glikson, 2006). The onset of detrital sedimentation following the 3.26 Ga and 3.24 Ga impacts suggests enhanced high-energy sedimentation derived from rejuvenated source terrains, possibly due to impact-triggered seismic faulting. Mantle isotopic signatures recorded in banded iron formations of the Hamersley Basin include positive εNd, values (+1.0±0.5) whereas associated shale bands yield mixed continental–oceanic εNd signatures (−0.9±0.6; Alibert and McCulloch, 1993). Iron isotope $^{56}Fe/^{54}Fe$ signatures tend to cluster about the igneous field, with departures attributed to diagenetic changes (Beard et al., 2003). Ge/Si trace element studies suggest alternation between volcanic or hydrothermal sources of the iron-rich bands and continental weathering sources of silica bands (Hamade et al., 2003). Decrease in carbonate sedimentation at the top of the Wittenoom Formation and onset of BIF/chert/argillite deposition of the Mount Sylvia and Mount McRae formations reflects chemical changes from high pH conditions of carbonate (+minor chert) precipitation to low pH conditions which allow transport of ferrous iron. However, intermittent carbonate sedimentation occurs above the Wittenoom Formation, including siderite-rich carbonate units intercalated with banded iron formations. Fluctuations between moderate Eh conditions, which allow oxidation of ferrous to ferric iron, and low Eh conditions required for deposition of reduced black shale, are manifest in the Mount Sylvia and Mount McRae formations. Microbial mediation of ferrous to ferric iron oxidation is supported by fine-scale stratigraphic correlations of iron–silica microbands throughout the Hamersley Basin (Trendall and Blockley, 1970; Cloud, 1973; Morris, 1993; Konhauser et al., 2002).

4. Discussion: Magmatic and tectonic consequences of mega-impacts

Correlations between the ages of large impact events and mafic igneous events are hampered by statistical imbalance, namely the large number of isotopically dated mafic igneous events as contrasted with the few known Precambrian impact events. Further, the mere overlap of isotopic ages does not provide sufficient evidence for genetic relationships between impact and volcanic events. The age of the SMB impact unit (2565±9 Ma; Trendall et al., 2004) overlaps the Sm–Nd 2586±16 Ma age of the Zimbabwe Great Dyke (Mukasa et al., 1998), but is marginally younger than U–Pb ages of the dyke (2587±8 Ma; Mukasa et al., 1998; 2578±0.9 Ma; Collerson et al., 2002), and Re–Os ages (2576±1 Ma; Schoenberg et al., 2003). The DGS4 (Dales Gorge Shale No. 4 Macroband) of the Brockman Iron Formation (Simonson, 1992; Glikson and Allen, 2004), dated at 2481±4 Ma and 2495±16 Ma (Trendall et al., 2004), and the correlated Kuruman Iron Formation in the Griqualand West Basin, South Africa (Simonson et al., 2006), occur about 37 m above the base of these banded iron formation sequences. Iridium mass-balance estimates of the ~20 cm-thick DGS4 suggest an asteroid diameter on the scale of ~20 kilometres (Fig. 8) (Glikson and Allen, 2004). An age overlap occurs between the DGS4 impact unit and onset of Huronian mafic igneous activity (2473+16/−9 Ma; Heaman, 1997), marking the onset of large-scale mafic dyke systems 2473–2446 Ma. The Matachewan-hearst dyke systems involve volumes of at least 50,000 km^3 of basaltic magma intruding an area >250,000 km^2 large (Halls and Bates, 1990). Remnants of a global ~2.50–2.42 Ga magmatic province are identified in many Archaean cratons, including the ~2.42 Ga Scourie dike swarm (Scotland), ~2.45–2.44 Ga Karelian layered mafic intrusions, flood basalts, and dike swarms (Finland and Russia), ~2.42 Ga Widgiemooltha dike swarm and Jimberlana intrusion (Western Australia), dyke systems in the Vestfold Craton (Antarctica) and the ~2.42 Ga Bangalore dike swarm (Dharwar Craton, India). The temporal coincidence of the ~2.48 Ga-old Dales (DGS4)-Kuruman asteroid mega-impact with the onset of global dyking events 2.48–2.42 Ga may be interpreted in terms of impact-induced crustal fracturing.

To date suggested cause–effect relations between large asteroid/comet impacts and igneous, tectonic or plate tectonic events (Price, 2001; Green, 1981; Grieve, 1980; Hughs et al., 1977; Jones, 1987; Jones et al., 2002; Jones et al., 2005; Alt et al., 1988; Oberbeck et al., 1992; Boslough et al., 1994; Glikson, 2001; Glikson, 2005; Glikson, 2006; Ingle and Coffin, 2004; Ivanov and Melosh, 2003; Glikson et al., 2004a,b; Elkin-Tanton et al., 2004; Elkin-Tanton and Hager, 2005; Abbott and Isley, 2002) have not been accompanied with field evidence. Ivanov and Melosh (2003) placed constraints on the likelihood of impact-triggered volcanic activity, referring to it as a rare coincidence in Earth history. However, these authors also state: "Indeed, a few giant impact events certainly occurred on Earth in post-LHB history, and a few might have encountered the fortuitous circumstances necessary for them to enhance magma production." (in Glikson et al., 2004b). The likelihood

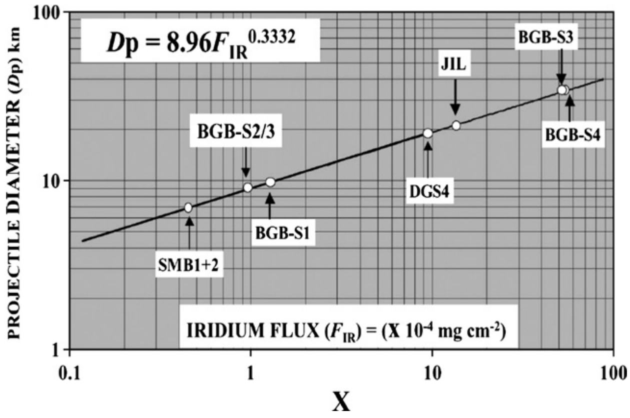

Fig. 8. Correlation between Ir flux (in units of 10^{-4} mg cm^{-2}) and diameter of chondritic projectile (Dp), based on mass-balance calculations assuming mean unit thickness, mean Ir concentration, and global distribution of ejecta. Unit symbols: Rp (projectile radius) = $\sqrt{[Vp/(4/3)\pi]}$; Vp = Mp / dp; Mp = FG / Cp; FG Earth = AE / dS × TS × S_{Earth} (Earth's surface area), where AE is measured element (*E*) abundance in ejecta unit (in ppb); dS is mean density of ejected materials (mg/cm^3) (assumed as 2.65 g/cm^3); CE = mass of element *E* (in mg/cm^3); (CE = AE × DS); TS = mean stratigraphic thickness of spherule unit (in mm); FE = local mean flux of element *E* (in mg per cm^2 surface; FE = CE × TS); FG = inferred global flux (in mg/cm^2) of element E; Cp = assumed concentration of element *E* in projectile (ppb) (C1 chondrites have 450 ppb Ir); Mp = mass of projectile; dp = assumed density of projectile (C1 chondrites' density = 3.0 g/cm^3).

of impact-triggered melting is increased in geothermally active oceanic crustal regions. For an impact flux of craters of Ds > 20 km (Ds = outer diameter) in the order of 4.3–6.3.10^{-15} km^{-2} yr^{-1} (Shoemaker and Shoemaker, 1996) on a post-3.8 Ga Earth occupied by >80% time-integrated oceanic crust (McCulloch and Bennett, 1994), for a cumulative asteroid and crater size/frequency distribution ND α D$10^{-1.8}$ (ND = number of craters of diameter *D*), some 360 craters with *D* > 100 km and some 40 craters with *D* > 300 km would form in oceanic basins (Glikson, 2001). A steeper size/frequency distribution of ND α D$10^{-2.2}$ (Neukum et al., 2001) would result in 125–250 craters of *D* > 100 km and 6–12 craters of *D* > 300 km. The more conservative estimate implies that, in so far as the 3.26 Ga, 3.24 Ga, 2.63 Ga, 2.56 Ga, 2.48 Ga, 2.03 Ga (Vredefort) and 1.85 Ga (Sudbury) impacts correspond to craters of *D* ≥ 300 km, the majority of very large impact structures on Earth has at this stage been recorded.

For a present-day mid-ocean geotherm (25 °C km^{-1}) occupying ~10% of oceanic crust, assuming yet higher Archaean geothermal gradients and possibly smaller-scale convection cells and plate dimensions (Lambert, 1983), thin (<5 km) crustal regions underlain by shallow asthenosphere (<50 km) can be expected to have occupied perhaps a quarter of the oceanic crust. Low-angle impacts in the deep ocean will be partly to largely absorbed by the water column. A high-angle impact by a ~20 km-diameter projectile on thin oceanic crust underlying <2 km water depth would ensue in a 300±100 km-diameter submarine crater. As originally modelled (Price, 2001; Green, 1981), downward compression of the transient crater followed by rebound of asthenosphere originally located at ~40–50 km would result in intersection of the peridotite solidus

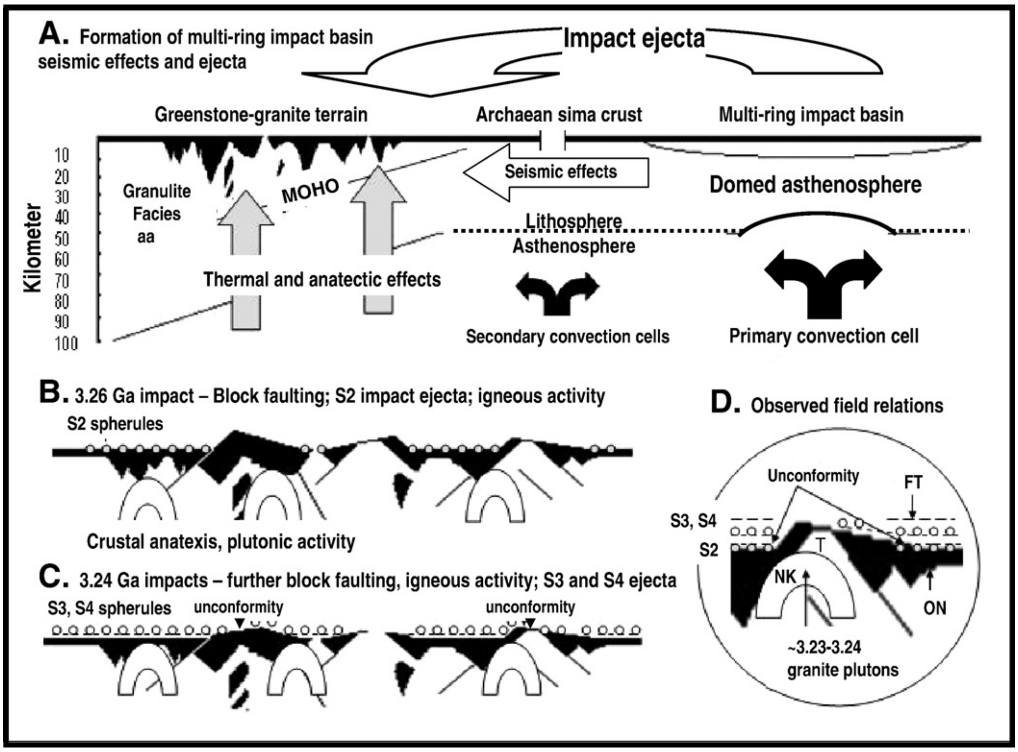

Fig. 9. A schematic model (not to scale) portraying the principal stages in asteroid impact-triggered cratering in simatic region of the Archaean Earth and ensuing rearrangement of mantle convection patterns, seismic activity, faulting, uplift, formation of unconformities and igneous activity in an affected greenstone-granite terrain. (A) 3.26 Ga — S2 impact: formation of a multi-ring impact basin by a 20 km asteroid impact, impact ejecta S2, seismically triggered faulting, mantle convection underlying impact basin, secondary mantle cells, thermal and anatectic effects across the asthenosphere/lithosphere boundary and the MOHO below greenstone-granite nuclei. (B) 3.26 Ga: Block faulting in greenstone-granite nuclei, rise of anatectic granites, S2 spherules preserved in below-wave base environments. (C) 3.24 Ga — S3 and S4 impacts, ejecta fallout over below-wave base S2 ejecta and overlying sediments and over unconformities. Further faulting, block movements and rise of plutonic magmas. (D) Schematic representation of observed field relations between the ~3.55–3.26 Ga mafic–ultramafic volcanic Onverwacht Group (ON), intrusive early tonalites and trondhjemites (T), 3.26–3.24 Ga granites (NK), S2 ejecta, unconformity, S3, S4 ejecta, and the Fig Tree Group sediments (FT).

by rising mantle diapers and in rapid partial melting. In so far as morphometric estimates (Grieve and Pilkington, 1996) may apply to asthenospheric uplift, the amount of rebound may be similar to that of a central uplift $SU=0.086Ds^{1.03}$, namely ~30 km. However, such large degrees rebound, deduced from craters formed in high-viscosity crust, may not apply to dense low-viscosity asthenosphere.

Elkin-Tanton et al. (2004), Elkin-Tanton and Hager (2005) modelled the magmatic consequences of very large impacts, suggesting that a 300 km-radius crater excavating 75 km-thick lithosphere will produce 10^6 km^3 magma through instantaneous in-situ decompression of the mantle and updoming of the asthenosphere, triggering longer-term mantle convection and adiabatic melting, in particular under high geothermal gradients. These volumes are similar to those estimated elsewhere (Ivanov and Melosh, 2003). The short eruption spans of large volumes of basalt in some instances (Decan: 2.10^6 km^3 in 0.3 Ma; Emeishan: 9.10^5 km^3 in 0.3 Ma; Siberian: $3–4.10^6$ km^3 in 0.4 Ma) are consistent with volumes deduced by these authors for excavation of large-radii impact craters. Impacts of this magnitude will have world-wide effects for which “ample evidence could remain in the rock record.” (Elkin-Tanton and Hager, 2005).

Ingle and Coffin (2004) suggested a possible impact origin for the short-lived ~120 Ma Ontong Java Plateau (OJP). Jones et al. (2002) and Jones et al. (2005) conducted hydrocode simulations to test whether impact-triggered volcanism is consistent with the OJP, using dry lherzolite melting parameters, a steep oceanic geotherm and a vertical incidence by a dunite projectile (diameter 30 km: velocity 20 km/s). The thermal and physical states of target lithosphere are critical for estimates of melt production. Model calculations suggest impact-triggered melting in a sub-horizontal disc of ~600 km-diameter down to >150 km depth in the upper mantle forms within ~10 min of the impact, whereas most of the initial melt forms at depths shallower than ~100 km. The volume of ultramafic melt would reach ~2.5 10^6 km^3, ranging from superheated melts within 100 km of ground zero to partial melting with depth and distance. The total melt volume would reach ~7.5×10^6 km^3 of basalt if heat was distributed to produce 20–30% partial mantle melting.

The juxtaposition of S2–S4 Barberton impacts with the fundamental boundary between the ~3.55–3.26 Ga Onverwacht mafic–ultramafic volcanic sequence and the overlying Fig Tree Group association of turbidite–felsic volcanic-banded iron formation provides the first direct evidence for major tectonic–magmatic effects of large impacts in terrestrial history. The evidence suggests that the 3.26–3.24 Ga impact cluster resulted in an abrupt termination of the protracted evolution of greenstone-TTG (tonalite–trondhjemite–granodiorite) systems, faulting, vertical movements and unconformities, and was accompanied by peak volcanic activity of the Sulphur Springs Group and peak plutonic events in both the Kaapvaal Craton (Nelshoogte and Kaap Valley plutons) and the Pilbara Craton (Cleland plutonic suite). The full scale of the ~3.26–3.24 Ga bombardment may not have been identified to date and the 3 recorded impact units may represent a minimum number. Iridium and chrome isotope-based mass-balance calculations, spherule size analysis and the ferromagnesian composition of the impact ejecta suggest asteroids about 20–50 km-diameter (Byerly and Lowe, 1994; Shukolyukov et al., 2000; Kyte et al., 2003), resulting in impact basins in the range of 200–1000 km-diameter, excavated in mafic–ultramafic crustal regions of the Archaean Earth. A model consistent with these parameters and experimental petrology (Price, 2001; Green, 1981) is summarized in Fig. 9 in the following terms:

1. For an high-angle impact by a 20 km-diameter [Dp] asteroid, a transient crater ~200 m in diameter and about 30 km depth [d = 1.5Dp] would form, penetrating through oceanic crust and part of the shallow (~50 km) lithosphere, followed by rebound ensuing in a complex crater of ~200–400 km diameter.
2. For geothermal gradients in the range of 12–25 °C/km, the lithosphere–asthenosphere boundary, located about 100–50 km depth, would be compressed downward by explosion of the bolide, followed by domal rebound and adiabatic melting producing volumes of ultramafic–mafic magma in the order of several 10^6 km^3 (Jones, 1987; Jones et al., 2002; Elkin-Tanton et al., 2004). The origin of adiabatic melting paths depends on both the geotherm and water content of mantle peridotite.
3. Melting takes place in 3 modes: A — shock vaporization and melting of the projectile and associated crater materials; B — decompression melting of crust and mantle; C — triggering of asthenospheric convection (Elkin-Tanton and Hager, 2005). Modes A and B are of mainly local to regional significance. However, impact by an asteroid >20 km in diameter may have wider significance through triggering and rearrangement of mantle asthenosphere convection patterns on a regional to global scale (Fig. 9).
4. Initial effects of impact by a >20 km-diameter asteroid on thin oceanic crust on neighbouring and distal greenstone-granite nuclei would include seismic-triggered faulting, fall-out of ejecta and tsunami. Triggering and reorganization of mantle convection cells would be reflected by mafic to ultramafic volcanic activity, enhanced geothermal gradients, crustal anatexis producing felsic volcanic and plutonic magma, faulting, uplift and resulting unconformities.
5. The thermal and igneous effects consequent on rearrangement of mantle convection systems would affect greenstone-granite nuclei. Block faulting, uplift and exposure of deep crustal levels would result in erosion, represented by unconformities, and in high-energy sedimentation, including turbidite and rudite. Exposure and denudation of mafic volcanic sequences, and possibly of impact-triggered mafic volcanics, would result in enrichment of sea water in ferrous iron under the low oxygen conditions of the Archaean hydrosphere and atmosphere.

These model predictions are consistent with field relationships in the Barberton Greenstone Belt and correlated stratigraphy in the central and western Pilbara Craton, as follows:

(1) ~3.255 Ga unconformable sediments and felsic volcanics of the Leilira Formation are succeeded with major mafic and ultramafic volcanic activity of the Sulphur Springs Group;
(2) major faulting ~3235 Ma is evident from olistostromes in the Sulphur Springs area;
(3) unconformities at the base of the S3 impact unit in the Barberton Greenstone Belt cut deep into the underlying Onverwacht Group (Lowe et al., 2003);
(4) plutonic granitoids of the Nelshoogte granite, Kaap Valley granite and Cleland granite suite correlate with the 3.26–3.24 Ga time span.

The field evidence militates for major tectonic movements and igneous events concomitant with, and likely genetically related to, Eros-scale impacts on the Archaean and early Proterozoic Earth.

Acknowledgements

I thank John Vickers for his contribution to the field and laboratory research, the Geological Survey of Western Australia for logistic and scientific support of my field research, and Arthur Hickman, Martin Van Kranendonk, Gary Byerly and Don Lowe for their comments on this manuscript.

References

Abbott, D.H., Isley, A.E., 2002. Extraterrestrial influences on mantle plume activity. Earth Planet. Sci. Lett. 205, 53–62.
Alibert, C., McCulloch, M.T., 1993. Rare earth element and neodymium composition of the banded iron-formations and associated shales from Hamersley, Western Australia. Geochim. Cosmochim. Acta 57, 187–204.
Alt, A.D., Sears, J.W., Hyndman, D.W., 1988. Terrestrial maria: the origins of large basalt plateaus, hotspot tracks and spreading ridges. J. Geol. 96, 647–662.
Arndt, N.T., Nelson, D.R., Compston, W., Trendall, A.F., Thorne, A.M., 1991. The age of the Fortescue Group, Hamersley Basin, Western Australia, from ion microprobe zircon U–Pb results. Aust. J. Earth Sci. 38, 261–281.
Beard, B.L., Johnson, C.M., Skulan, J.L., Nealson, K.H., Cox, L., Dun, H., 2003. Application of Fe isotopes to tracing the geochemical and biological cycling of Fe. Chem. Geol. 195, 87–117.
Boslough, M.B., Chael, E.P., Trucano, T.G., Kipp, M.E., Crawford, D.A., 1994. Axial focussing of impact energy in the Earth's interior: proof-of-principle tests of a new hypothesis. Lun. Planet. Institut. Contr. 825, 14–15.
Buick, R., Brauhart, C.A.W., Morant, P., Thornett, J.R., Maniew, J.G., Archibald, J.G., Doepel, M.G., Fletcher, I.R., Pickard, A.L., Smith, J.B., Barley, M.B., McNaughton, N.J., Groves, D.I., 2002. Geochronology and stratigraphic relations of the Sulphur Springs Group and Strelley Granite: a temporally distinct igneous province in the Archaean Pilbara Craton, Australia. Precamb. Res. 114, 87–120.
Byerly, G.R., Lowe, D.R., 1994. Spinels from Archaean impact spherules. Geochim. Cosmochim. Acta 58, 3469–3486.
Byerly, G.R., Lowe, D.R., Wooden, J.L., Xiaogang, X., 2002. A meteorite impact layer 3470 Ma from the Pilbara and Kaapvaal Cratons. Science 297, 1325–1327.
Cloud, P., 1973. Paleoecological significance of the banded iron formation. Econ. Geol. 68, 1135–1143.

Collerson, K.D., Kamber, B.S., Schoenberg, R., 2002. Applications of accurate, high-precision Pb isotope ratio measurement by multi-collector ICP-MS. Chem. Geol. 188, 65–83.

Elkin-Tanton, L.T., Hager, T.L., 2005. Giant meteoroid impacts can cause volcanism. Earth Planet. Sci. Lett. 239, 219–232.

Elkin-Tanton, L.T., Hager, B.H., Grove, T.L., 2004. Magmatic effects of the lunar late heavy bombardment. Earth Planet. Sci. Lett. 222, 17–27.

Glass, B.P., Burns, C.A., 1988. Microkrystites: a new term for impact-produced glassy spherules containing primary crystallites. Proc.Lun. Planet. Sci.18th 455–458.

Glikson, A.Y., 2004. Early Precambrian asteroid impact-triggered tsunami: excavated seabed, debris flows, exotic boulders, and turbulence features associated with 3.472 Ga-old asteroid impact fallout units, Pilbara Craton, Western Australia. Astrobiology 4, 19–50.

Glikson, A.Y., 2001. The astronomical connection of terrestrial evolution: crustal effects of post-3.8 Ga mega-impact clusters and evidence for major 3.2 ± 0.1 Ga bombardment of the Earth–Moon system. J. Geodyn. 32, 205–229.

Glikson, A.Y., 2006. Asteroid impact ejecta units overlain by iron-rich sediments in 3.5–2.4 Ga terrains, Pilbara and Kaapvaal cratons: accidental or cause–effect relationships? Earth Planet. Sci. Lett. 246, 149–160.

Glikson, A.Y., 2005. Geochemical signatures of Archaean to early Proterozoic maria-scale oceanic impact basins. Geology 35, 125–129.

Glikson, A.Y., 2007. Siderophile element patterns, PGE nuggets and vapour condensation effects in Ni-rich quench chromite-bearing microkrystite spherules, 3.24 Ga S3 impact unit, Barberton Greenstone Belt, Kaapvaal Craton, South Africa. Earth Planet. Sci. Lett. 253, 1–16.

Glikson, A.Y., Allen, C., 2004. Iridium anomalies and fractionated siderophile element patterns in impact ejecta, Brockman Iron Formation, Hamersley Basin, Western Australia: evidence for a major asteroid impact in simatic crustal regions of the early Proterozoic earth. Earth Planet. Sci. Lett. 220, 247–264.

Glikson, A.Y., Vickers, J., 2006. The 3.26–3.24 Ga Barberton asteroid impact cluster: tests of tectonic and magmatic consequences, Pilbara Craton, Western Australia. Earth Planet. Sci. Lett. 241, 11–20.

Glikson, A.Y., Allen, C., Vickers, J., 2004a. Multiple 3.47-Ga-old asteroid impact fallout units, Pilbara Craton, Western Australia. Earth Planet. Sci. Lett. 221, 383–396.

Glikson, A.Y., Ivanov, B., Melosh, H.J., 2004b. Discussion of "Impacts do not initiate volcanic eruptions: Eruptions close to the crater". Geology Online Forum e47–e48.

Green, D.H., 1981. Petrogenesis of Archaean ultramafic magmas and implications for Archaean tectonics. In: Kroner, A. (Ed.), Precambrian Plate Tectonics. Elsevier, Amsterdam, pp. 469–489.

Grieve, R.A.F., 1980. Impact bombardment and its role in proto-continental growth of the early Earth. Precamb. Res. 10, 217–248.

Grieve, R.A.F., Pilkington, M., 1996. The signature of terrestrial impacts. Aust. Geol. Surv. Org. J. Aust. Geol. Geophys. 16, 399–420.

Halls, H.C., Bates, M.P., 1990. The evolution of the 2.45 Ga Matachewan dike swarm. In: Parker, A.J., et al. (Ed.), Mafic Dikes and Emplacement Mechanisms. Balkema, Canada, pp. 237–249.

Hamade, T., Konhauser, K.O., Raiswell, R., Goldsmith, S., Morris, R.C., 2003. Using Ge/Si ratios to decouple iron and silica fluxes in Precambrian banded iron formations. Geology 31, 35–38.

Hassler, S.W., Simonson, B.M., Sumner, D.Y., Murphy, D., 2005. The sedimentary record of extraterrestrial impacts in deep shelf environments: evidence from the early Precambrian. Aust. J. Earth Sci. 52, 759–772.

Heaman, L.M., 1997. Global mafic magmatism at 2.45 Ga: remnants of an ancient large igneous province? Geology 25, 299–302.

Hill, R.M., Stratigraphy, structure and alteration of hanging wall sedimentary rocks at the Sulphur Springs volcanogenic massive sulphide (VMS) prospect, east Pilbara Craton, Western Australia, B.Sc Hon.Thesis, Univ. W. Aust. (1977) 67 pp.

Hughs, H.G., App, F.N., McGetchin, T.N., 1977. Global seismic effects of basin-forming impacts. Phys. Earth Planet. Inter. 15, 251–263.

Ingle, S., Coffin, M.F., 2004. Impact origin for the greater Ontong Java Plateau? Earth Planet. Sci. Lett. 18, 123–134.

Ivanov, B.A., Melosh, H.J., 2003. Impacts do not initiate volcanic eruptions: eruptions close to the crater. Geology 31, 869–872.

Jones, A.G., 1987. Are impact-generated lower crustal faults observable? Earth Planet. Sci. Lett. 85, 248–252.

Jones, A.P., Price, G.D., DeCarli, P.S., Price, N.J., Clegg, R., 2002. Impact induced melting and the development of large igneous provinces. Earth Planet. Sci. Lett. 202, 551–561.

Jones, A.P., Wünemann, K., Price, G.D., 2005. Modeling impact volcanism as a possible origin for the Ontong Java Plateau. Geol. Soc. Am. Sp. Pap. 388, 711–720.

Konhauser, K.O., Hamada, T., Raiswell, R., Morris, R.C., Ferris, F., Southam, G., Canfield, D., 2002. Could bacteria have formed the Precambrian banded iron-formations? Geology 30, 1079–1082.

Kyte, F.T., Shukolyukov, A., Lugmair, G.W., Lowe, D.R., Byerly, G.R., 2003. Early Archaean spherule beds: chromium isotopes confirm origin through multiple impacts of projectiles of carbonaceous chondrite type. Geology 31, 283–286.

Lambert, R.S.t.J., 1983. Metamorphism and thermal gradients in the Proterozoic continental crust. Geol. Soc. Am. Mem. 161, 155–166.

Lowe, D.R., Byerly, G.R., 1990. Direct determination of the environmental effects of large meteorite impacts on the Archaean Earth. EOS 71, 1429–1430.

Lowe, D.R., Nocita, B.W., 1999. Foreland basin sedimentation in the Mapepe Formation, southern-facies Fig Tree Group. Spec. Pap. Geol. Soc. Am. 329, 233–258.

Lowe, D.R., Byerly, G.R., Asaro, F., Kyte, F.T., 1989. Geological and geochemical record of 3400 million years old terrestrial meteorite impacts. Science 24, 959–962.

Lowe, D.R., Byerly, G.R., Kyte, F.T., Shukolyukov, A., Asaro, F., Krull, A., 2003. Spherule beds 3.47–3.34 Ga-old in the Barberton Greenstone Belt, South Africa: a record of large meteorite impacts and their influence on early crustal and biological evolution. Astrobiology 1, 7–48.

McCulloch, M.T., Bennett, V.C., 1994. Progressive growth of the Earth's continental crust and depleted mantle: geochemical constraints. Geochim. et Cosmochim. Acta 58, 4717–4738.

Morris, R.C., 1993. Genetic modelling for banded iron-formation of the Hamersley Group, Pilbara Craton, Western Australia. Precam. Res. 60, 243–286.

Mukasa, S.B., Wilson, A.H., Carlson, R.W., 1998. A multi-element geochronological study of the Great Dyke, Zimbabwe: significance of the robust and reset ages. Earth Planet. Sci. Lett. 164, 353–369.

Neukum, G., Ivanov, B., Hartmann, W.K., 2001. Cratering records in the inner solar system. In: Kallenbach, R., et al. (Ed.), Chronology and Evolution of Mars. Dordrecht, Kluwer, pp. 55–86.

Oberbeck, V.R., Marshall, J.R., Aggarval, H., 1992. Impacts, tillites and the breakdown of Gondwanaland. J. Geol. 101, 1–19.

Price, N.J., 2001. Major Impacts and Plate Tectonics; A Model for the Phanerozoic Evolution of the Earth's Lithosphere. Taylor and Francis, London. 416 pp.

Rasmussen, B., Blake, T.S., Fletcher, I.R., 2005. U–Pb zircon age constraints on the Hamersley spherule beds: evidence for a single 2.63 Ga Jeerinah–Carawine impact ejecta layer. Geology 33, 725–728.

Schoenberg, R., Nägler, T.h.F., Gnos, E., Kramers, J.D., Kamber, B.S., 2003. The source of the great dyke, Zimbabwe, and its tectonic significance: evidence from Re–Os isotopes. The Journal of Geology 111, 565–578.

Shoemaker, E.M., Shoemaker, C.S., 1996. The Proterozoic impact record of Australia. Aust. Geol. Surv. Org. J. Aust. Geol. Geophys. 16, 379–398.

Shukolyukov, A., Kyte, F.T., Lugmair, G.W., Lowe, D.R., Byerly, G.R., 2000. The oldest impact deposits on Earth, Impacts and the Early Earth, in: Impacts and the Early Earth. In: Koeberl, C., Gilmour, I. (Eds.), Springer-Verlag, Berlin, pp. 99–116.

Simonson, B.M., 1992. Geological evidence for an early Precambrian microtektite strewn field in the Hamersley Basin of Western Australia. Geol. Soc. Am. Bull. 104, 829–839.

Simonson, B.M., Hassler, S.W., 1997. Revised correlations in the early Precambrian Hamersley Basin based on a horizon of resedimented impact spherules. Aust. J. Earth Sci. 44, 37–48.

Simonson, B.M., Glass, B.P., 2004. Spherule layers — records of ancient impacts. Ann. Rev. Earth Planet. Sci. 32, 329–361.

Simonson, B.M., Davies, D., Hassler, S.W., 2000. Discovery of a layer of probable impact melt spherules in the late Archean Jeerinah Formation, Fortescue Group, Western Australia. Aust. J. Earth Sci. 47, 315–325.

Simonson, B.M., Sumner, D.Y., Beukes, N.J., Hassler, S.W., Kohl, I., Jones-Zimberlin, S., Johnson, S., Scally, A., Gutzmer, J., 2006. Correlating multiple Neoarchaean–Palaeoproterozoic impact spherule layers between South Africa and Western Australia. Lunar Planet. Sci. XXXVII (1489) pdf.

Trendall, A.F., Blockley, J.G., 1970. The iron-formations of the Precambrian Hamersley Group, Western Australia: with special reference to associated crocidolite. Bull.-Geol. Surv. West. Aust. 119 336 pp.

Trendall, A.F., Compston, W., Nelson, D.R., deLaeter, J.R., Bennett, V.C., 2004. SHRIMP zircon ages constraining the depositional chronology of the Hamersley Group, Western Australia. Aust. J. Earth Sci. 51, 621–644.

Van Kranendonk, M.J. Geological Survey of Western Australia 1:100 000 Geological Series Explanatory Notes North Shaw 1:100 000 Sheet (2000) 86 pp.

Van Kranendonk, M.J., Hickman, A.H., Smithies, R.H., Nelson, D.R., 2002. Geology and tectonic evolution of the Archaean North Pilbara Terrain, Pilbara Craton, Western Australia. Econ. Geol. 97, 695–732.

Van Kranendonk, M.J., Smithies, R.H., Hickman, A.H., Bagas, L., Williams, I.R., Farrell, T.R., 2005. Geological Survey of Western Australia Annual Report for 2004, pp. 49–61.

Van Kranendonk, M.J., Hickman, A.H., Smithies, R.H., Williams, I.R., Bagas, L., Farrell, T.R., 2006. Geological Survey of Western Australia Record 2006/15.